Hybrid plasmon polariton guiding with tight mode confinement in a V-shaped metal/dielectric groove

2013 J. Opt. 15 055011

(http://iopscience.iop.org/2040-8986/15/5/055011)

IOP PUBLISHING JOURNAL OF OPTICS
J. Opt. **15** (2013) 055011 (6pp) doi:10.1088/2040-8978/15/5/055011

Hybrid plasmon polariton guiding with tight mode confinement in a V-shaped metal/dielectric groove

Yusheng Bian[1], Zheng Zheng[1], Xin Zhao[1], Lei Liu[1], Yalin Su[1], Jiansheng Liu[1], Jinsong Zhu[2] and Tao Zhou[3]

[1] School of Electronic and Information Engineering, Beihang University, Beijing 100191, People's Republic of China
[2] National Center for Nanoscience and Technology, No.11 Zhongguancun Beiyitiao, Beijing 100190, People's Republic of China
[3] Department of Physics, New Jersey Institute of Technology, Newark, NJ 07102, USA

E-mail: zhengzheng@buaa.edu.cn

Received 25 December 2012, accepted for publication 22 March 2013
Published 17 April 2013
Online at stacks.iop.org/JOpt/15/055011

Abstract
Plasmonic waveguides consisting of metallic grooves filled with low- and high-index dielectrics are proposed and the optical properties of guided plasmonic modes are investigated at a wavelength of 1550 nm. Numerical simulations reveal that the quasi-TE-like fundamental hybrid plasmonic mode exhibits strong localization near the low-index dielectric gap, along with pronounced local field enhancement and relatively small mode area. Moderate propagation loss can be achieved as well, corresponding to a propagation distance of around tens to hundreds of microns. The proposed hybrid plasmonic structure is compatible with the fabrication techniques of traditional channel plasmon polariton waveguides, and these structures could be employed as interesting building blocks for highly integrated photonic circuits.

Keywords: surface plasmons, photonic integrated circuits, guided waves, hybrid waveguides

(Some figures may appear in colour only in the online journal)

1. Introduction

The ever-increasing demand for continuous miniaturization of high-density photonic integrated circuits has motivated research into novel guiding schemes capable of manipulating light at the subwavelength scale [1]. Surface plasmons (SPs), coherent oscillations of the electron density at the metal/dielectric surface, have been utilized as promising candidates for subwavelength light guiding, due to their unique capability of effectively overcoming the diffraction limit existing in conventional photonics technology [2]. Among the previously studied surface plasmon polariton (SPP) structures for subwavelength light confinement and guiding, triangular metallic grooves supporting the propagation of channel plasmon polaritons (CPPs) have been intensively investigated for their capability of simultaneously providing tight light confinement and long propagation distance [3–7]. Another merit is their ease of fabrication, which has enabled a number of experimental demonstrations [8–12].

Conventional CPP waveguides are based on a sharp-angled groove milled on a metallic surface (near-infinite [5, 8] or finite thickness [13, 14]). The grooves are either exposed directly to air [5, 8] or filled with some kind of dielectric material [15, 16]. The fundamental plasmonic mode supported by a near-infinite metal groove with an air cladding exhibits a quasi-TE-like behavior and becomes highly confined at the bottom corner of the channel at optical frequencies, while it shifts towards the groove opening with increased wavelength [17]. The propagation distance of the CPP mode can reach 100 μm; however, the

corresponding mode confinement is relatively weak, with the mode size approaching the wavelength scale. In this paper, in order to realize subwavelength mode confinement and low propagation loss simultaneously, we look into an alternative structure consisting of a metal groove waveguide filled with different materials, i.e. more than one material inside the grooves. It is found that the associated modal properties would be greatly modified due to the incorporation of the hybrid material. For a groove filled with two types of dielectric (with high-index contrast), the strong coupling between the triangular high-index dielectric core and the metallic wall results in a novel hybrid plasmonic mode featuring both strong confinement and long-range propagation length, similar to other hybrid plasmonic waveguides [18–27]. Besides, such a structure can be realized using fabrication techniques similar to those of conventional CPP [8] and wedge plasmon polariton (WPP) waveguides [28]. For example, one of the possible approaches to form a hybrid groove is based on the conventional CPP structure, which can be implemented by first milling a V-shaped groove onto a metal substrate, followed by subsequent deposition of the low-index and high-index materials. Another feasible method is by employing totally reversed steps. After formation of a low-index dielectric coated high-index dielectric ridge, the metal cladding is deposited onto the whole structure. In the following discussion, the present hybrid structure is denoted as a channel hybrid plasmonic waveguide for convenience. Detailed investigation of the properties of the fundamental hybrid plasmonic modes with changes of key geometric parameters is carried out at the telecom wavelength.

2. Analysis of the channel hybrid plasmonic waveguide

Figure 1 shows a schematic of the proposed channel hybrid plasmonic waveguide, where a triangular upside-down high-index dielectric wedge is incorporated inside the metal groove, with a homogeneously thick low-index dielectric filling the gap between the groove and the wedge. The bottom angle of the metal groove is θ, which is the same as that of the high-index wedge. The depth of the metal groove is h while the top width of the dielectric wedge is w. The low-index dielectric layer has a uniform thickness t, which also dictates the gap width. The bottom corner of the wedge has a 10 nm curvature while the corresponding metal groove corner has a radius of $(10 + t)$ nm in order to maintain a constant gap width. Thus, the depth of the dielectric wedge equals $(h - t)$. The modal characteristics of the proposed waveguide are investigated at $\lambda = 1550$ nm by the finite-element method (FEM) using COMSOL^{TM}. The 2D eigenmode solver is used with the scattering boundary condition. Fine meshes with a maximum mesh size of around 2 nm are adopted in the low-index gap region, and 5 nm for the high-index wedge. Convergence tests are performed to ensure that the numerical boundaries and meshing do not interfere with the solutions. The cladding and the gap are made of silica (SiO_2), while the metal substrate is assumed to be silver (Ag) and the dielectric wedge is made of silicon (Si). The permittivities of Si, SiO_2 and Ag are $\varepsilon_d = 12.25$, $\varepsilon_c = \varepsilon_g = 2.25$ and $\varepsilon_m = -129 + 3.3i$ [18], respectively.

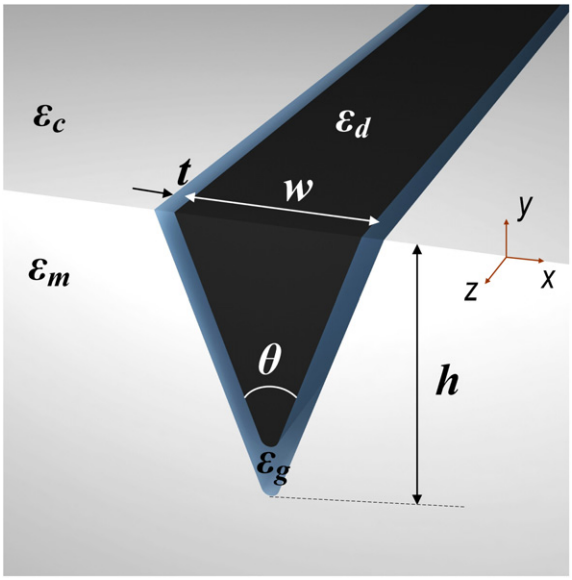

Figure 1. Schematic of the studied channel hybrid waveguide.

The electric field distribution of the fundamental quasi-TE hybrid plasmonic mode is shown in figure 2, where the groove angle is set at 25°, with $h = 500$ nm and $t = 20$ nm. From the 2D field panel, it is seen that the mode is tightly localized near the gap and the silicon ridge. Besides, pronounced local field enhancement is observable in the low-index silica gap, as shown in the cross-sectional field plots, along with reasonable modal overlap in the high-index silicon wedge, which is beneficial for potential applications in active components such as nanolasers. It is also seen that the enhancements are much more obvious in the upper part of the groove than in the bottom region, due to the stronger interaction between the upper silicon wedge and the metallic sidewalls.

Figures 3(a)–(c) demonstrate the dependence of the calculated modal properties of the fundamental quasi-TE hybrid mode on the groove depth h for different gap widths ($t = 10$ nm, 20 nm, 40 nm), where the groove angle is fixed at 25°. In the figures, n_{eff} is the real part of the modal effective index N_{eff}. The propagation distance is obtained by $L = \lambda/[4\pi \,\text{Im}(N_{\text{eff}})]$, whereas the effective mode area is calculated using

$$A_{\text{eff}} = \left(\iint W(\boldsymbol{r})\,\mathrm{d}A\right)^2 \Big/ \left(\iint W(\boldsymbol{r})^2\,\mathrm{d}A\right) \qquad (1)$$

where, to accurately account for the energy in the metal region, the electromagnetic energy density $W(r)$ is defined as [18]

$$W(\boldsymbol{r}) = \frac{1}{2}\text{Re}\left\{\frac{\mathrm{d}[\omega\varepsilon(r)]}{\mathrm{d}\omega}\right\}|E(\boldsymbol{r})|^2 + \frac{1}{2}\mu_0\,|H(r)|^2\,. \qquad (2)$$

In equation (2), $E(r)$ and $H(r)$ are the electric and magnetic fields, $\varepsilon(r)$ is the electric permittivity and μ_0 is the

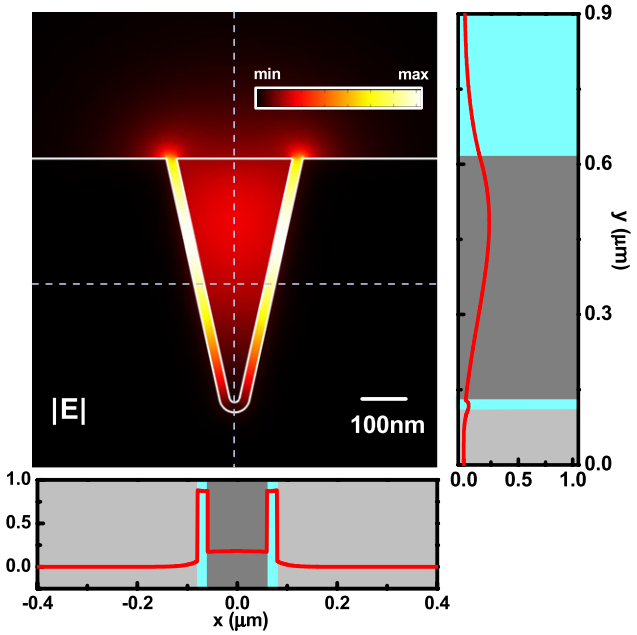

Figure 2. Electric field distribution of the fundamental quasi-TE plasmonic mode supported by the channel hybrid plasmonic waveguide ($\theta = 25°$, $h = 500$ nm, $t = 20$ nm). Normalized fields along the dashed lines in the 2D panel are also depicted to better illustrate the field enhancements in the silica gap.

vacuum magnetic permeability. A_0 is the diffraction-limited mode area in free space and is defined as $\lambda^2/4$. The normalized mode area is calculated using A_{eff}/A_0.

It is illustrated clearly in figure 3 that the fundamental quasi-TE mode for all of the three cases exhibits a cut off at a certain groove depth. A larger critical h (corresponding to a cut off) is observed for the structure with a wider gap width. The effective index approaches 1.5 (black dashed line in figure 3(a)) near the cut off due to the large portion of the field residing in the silica cladding, where both increased propagation length and expanded mode area are also observable (see figures 3(b) and (c)). Increase of the groove depth or decrease of the gap width could result in a monotonic increase in the modal effective index while leading to a more complex trend in the propagation distance and the mode area. Both L and A_{eff} decrease first before they increase, exhibiting thereby minimum values at certain groove depths. Such a phenomenon can also be found in other hybrid plasmonic waveguides [18, 25], which is an indication of strong coupling between the dielectric and plasmonic modes, resulting also in a relatively large amount of mode power stored inside the low-index silica gap region (see the corresponding electric field plot in the inset of figure 3(c)). An extended propagation length can be achieved by using even deeper metal grooves or employing larger gap widths, at the price of increased mode area correspondingly. As shown in figure 3, within the considered geometric parameter range, subwavelength mode confinement can be realized along with relatively large propagation distance (around tens to hundreds of microns), which makes the studied hybrid waveguides promising candidates for a number of potential applications.

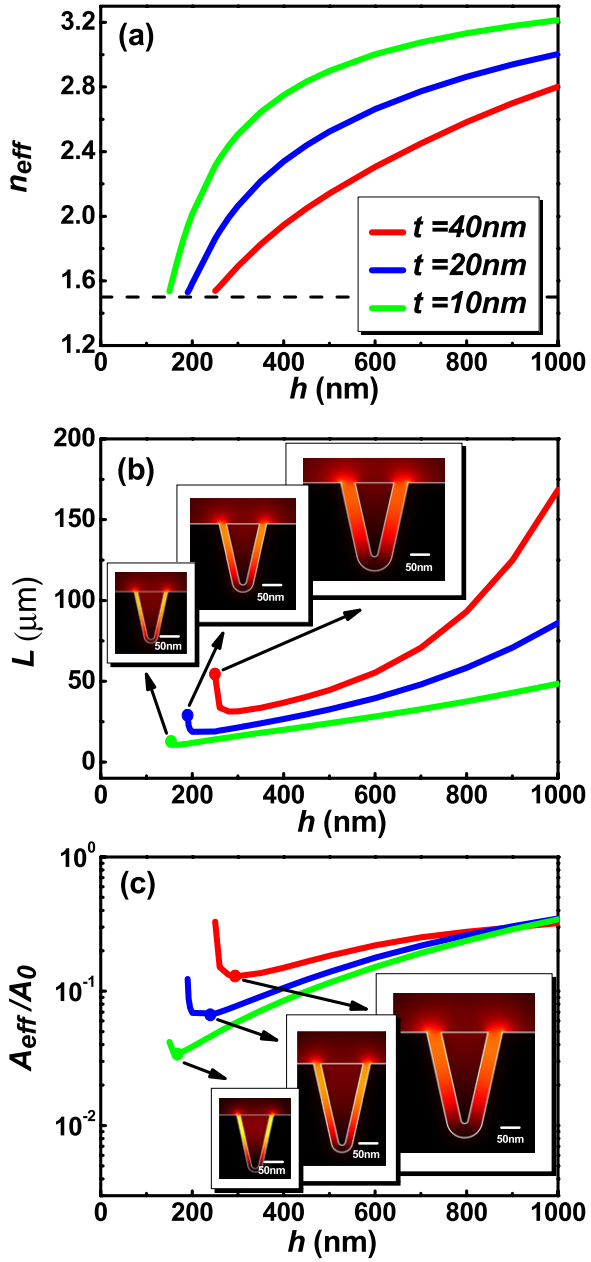

Figure 3. Dependence of the modal properties of the hybrid plasmonic mode on the groove depth ($\theta = 25°$): (a) modal effective index (n_{eff}); (b) propagation distance (L); (c) normalized mode area (A_{eff}/A_0). Red curve: $t = 40$ nm; blue curve: $t = 20$ nm; green curve: $t = 10$ nm. The dashed line in (a) corresponds to the refractive index of the silica cladding, i.e. 1.5. The insets plot the corresponding electric field distributions of the hybrid mode. In (b), from left to right: $h = 150$ nm, $t = 10$ nm; $h = 190$ nm, $t = 20$ nm; $h = 250$ nm, $t = 40$ nm. In (c), from left to right: $h = 160$ nm, $t = 10$ nm; $h = 250$ nm, $t = 20$ nm; $h = 300$ nm, $t = 40$ nm.

To further illustrate the mode confinement in different dielectric regions during variation of the waveguiding geometry, we now calculate the normalized optical powers (*NOPs*) in the silica gap and the silicon wedge. Here, *NOP* is defined as the ratio of the power inside the corresponding region to the total power of the waveguide. All the geometric parameters are chosen the same as those in figure 3. From

figure 4(a), it can be seen that, for each gap width, there exists an optimized NOP_{gap} with respect to the groove depth, which corresponds to the largest power ratio confined in the gap. This critical h shifts toward a larger value when the gap width increases, similarly to the change of the groove depth for minimal L and A_{eff} at different t (see figures 3(b) and (c)). A close comparison between figures 3 and 4 also reveals the fact that, for a specific gap width, the occurrence of minimal L (also A_{eff}) and maximal NOP_{gap} cannot be achieved simultaneously, i.e. the critical groove depths for the two conditions are different. Such a deviation may be caused by the geometrical changes in both the silicon wedge and the metal groove during the increase of h, which result in a more complicated coupling between the dielectric and plasmonic modes. Compared to the waveguide studied here, the hybridization of modes for the conventional hybrid plasmonic structure in [18] is relatively simple. As only the high-index dielectric varies its width during the geometric optimization, while the flat metallic surface remains unchanged, the variation of the coupling strength between the two modes can thus be attributed only to the change of the dielectric mode. From figure 4, it is also seen that when h is relatively small, the power located in the gap is not that large due to spreading of the field into the cladding. On the other hand, when h exceeds a certain value, NOP_{gap} drops gradually, with increased optical power concentrated in the high-index silicon wedge, as indicated in the curves of figure 4(b) and the corresponding field plot. In such cases, the hybrid mode behaves more like a dielectric mode, manifesting relatively low loss and large modal area. Such a power ratio could be further increased by adopting an even smaller gap width, which may be useful to facilitate gain when leveraged in active plasmonic devices. It is also worth mentioning that quasi-TM hybrid modes and other higher-order modes could also be supported by the structure at larger groove depth due to the hybridization between different plasmonic and dielectric modes.

Numerical simulations also reveal that the propagation loss of the quasi-TE hybrid plasmonic mode could be further reduced by increasing the curvature of the bottom corner of the Si wedge. For instance, considering a typical structure with a groove depth of 500 nm and a gap width of 20 nm, the propagation length is 32.6 μm for a Si wedge with a 10 nm curvature, while it increases to 64.7 μm when the curvature of the wedge reaches 100 nm. Furthermore, it is also shown that owing to the existence of the high-index silicon wedge near the metallic groove, the studied hybrid plasmonic mode could be supported by the proposed waveguide configuration within a much wider range of groove angles than the standard CPP waveguide case, similarly to the previously reported hybrid groove structures [29].

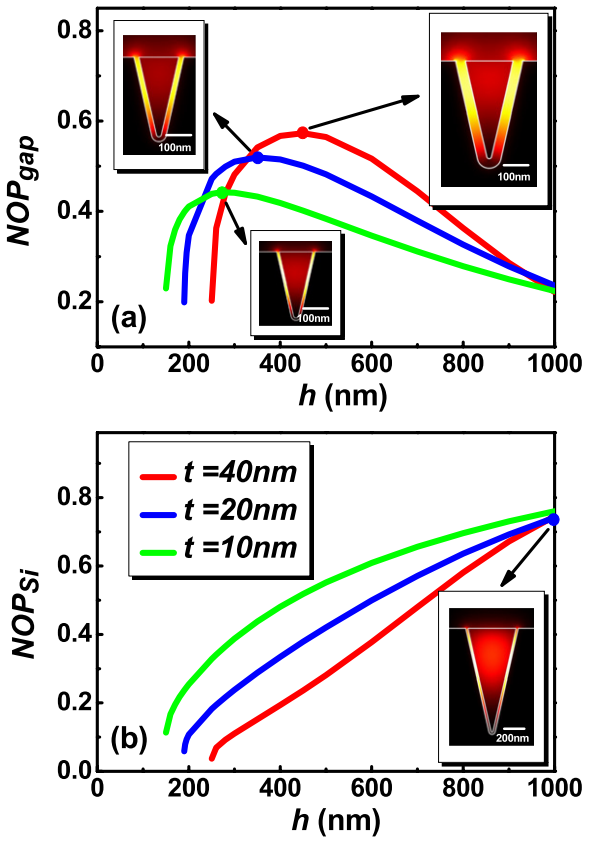

Figure 4. Optical power ratios in the silica gap and the silicon wedge of the hybrid mode: (a) normalized optical power in the gap (NOP_{gap}); (b) normalized optical power in the wedge (NOP_{si}). Red curve: $t = 40$ nm; blue curve: $t = 20$ nm; green curve: $t = 10$ nm. The insets plot the corresponding electric field distributions of the hybrid mode. In (a), upper insets, from left to right: $h = 350$ nm, $t = 20$ nm; $h = 450$ nm, $t = 40$ nm; lower insets: $h = 280$ nm, $t = 10$ nm. In (b), $h = 1000$ nm, $t = 20$ nm.

3. Comparisons between the channel hybrid waveguide and a CPP waveguide

To further benchmark the properties of the channel hybrid waveguide presented here, we make a quantitative comparison between the optical performance of the channel hybrid structure and a standard CPP waveguide. Here, the physical dimensions of the channel hybrid waveguide are set to be the same as those in the first set of simulations in figure 3. The CPP waveguide is also assumed to be made of silver for a fair comparison. The top and bottom corners of the groove are rounded with 100 nm and 10 nm curvatures, respectively [30]. In order to ensure the existence of a standard CPP mode, the groove depth is set at 1500 nm, with the groove angles chosen as 16° and 25°. 2D parameter plots of the normalized mode area (A_{eff}/A_0) versus the normalized propagation distance (L/λ) are introduced to allow for direct comparison of different properties. Here, for the proposed channel hybrid waveguide, by directly adopting the data from figures 3(b) and (c), we are able to show the relationship between the mode area and the propagation distance for different groove depths. It is illustrated in figure 5 that the standard CPP mode typically has a low transmission loss. For instance, its propagation distance can be more than 100 μm at 16° while exceeding 200 μm at 25°. However, the corresponding effective mode area is relatively large. By contrast, the presented channel hybrid waveguide is able to achieve a much smaller mode area, while still retaining a reasonable propagation distance,

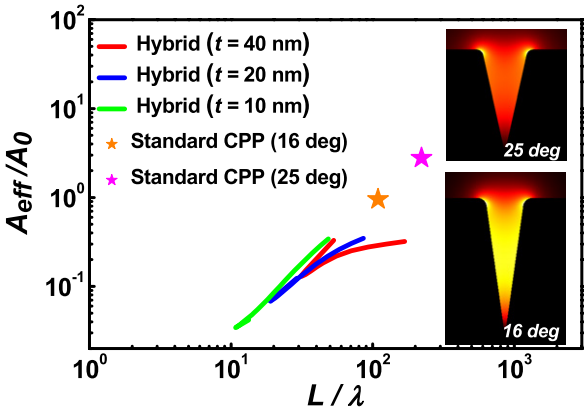

Figure 5. Performance comparison between the proposed channel hybrid waveguide and a standard CPP structure. The insets show the electric field distributions of the CPP modes supported by different geometries.

which makes it a better candidate for light guiding at the subwavelength scale.

Considering the excitation strategy, the guided mode of the channel hybrid waveguide can also be directly excited by using tapered optical fibers such as those applied in standard CPP structures, although its non-uniform field distribution might offer some challenges in achieving a relatively high launching efficiency. Besides, the hybrid mode could be launched by other dielectric modes as well. For instance, the proposed hybrid waveguide could be integrated with a standard silicon-on-insulator waveguide before connecting with an input fiber, similarly to approaches that are widely employed in experimental studies of many other silicon based plasmonic structures [26, 31].

Since tight optical confinement and significant local field enhancement can be achieved in the low-index gap of the channel hybrid waveguide, it offers interesting potential for various applications. However, there is a limitation of this structure when employed for sensing applications. As the metal groove has been completely filled, most of its mode field cannot be easily accessed. For this application, standard CPP structures would be better candidates than channel hybrid waveguides as their open grooves make them naturally behave as plasmonic sensors.

4. Conclusions

We have presented a novel plasmonic waveguide to provide tight confinement of light in the low-index gap region with long-range propagation length, simply by incorporating high-index contrast dielectric into the V-shaped metal grooves. The structure is also compatible with standard fabrication processes and could enable the realization of various plasmonic devices and photonic circuits.

Acknowledgments

This work was supported by 973 Program (2009CB930701), NSFC (61221061/61077064), National Key Scientific Instruments and Equipment Development Special Fund Management (2011YQ0301240502) and a Scholarship Award for Excellent Doctoral Student granted by the Ministry of Education at Beihang University.

References

[1] Kirchain R and Kimerling L 2007 A roadmap for nanophotonics *Nature Photon.* **1** 303–5
[2] Barnes W L, Dereux A and Ebbesen T W 2003 Surface plasmon subwavelength optics *Nature* **424** 824–30
[3] Pile D F P and Gramotnev D K 2004 Channel plasmon-polariton in a triangular groove on a metal surface *Opt. Lett.* **29** 1069–71
[4] Gramotnev D K and Pile D F P 2004 Single-mode subwavelength waveguide with channel plasmon-polaritons in triangular grooves on a metal surface *Appl. Phys. Lett.* **85** 6323–5
[5] Bozhevolnyi S I, Volkov V S, Devaux E and Ebbesen T W 2005 Channel plasmon-polariton guiding by subwavelength metal grooves *Phys. Rev. Lett.* **95** 046802
[6] Bozhevolnyi S I 2006 Effective-index modeling of channel plasmon polaritons *Opt. Express* **14** 9467–76
[7] Yan M and Qiu M 2007 Guided plasmon polariton at 2D metal corners *J. Opt. Soc. Am.* B **24** 2333–42
[8] Bozhevolnyi S I, Volkov V S, Devaux E, Laluet J Y and Ebbesen T W 2006 Channel plasmon subwavelength waveguide components including interferometers and ring resonators *Nature* **440** 508–11
[9] Volkov V S, Bozhevolnyi S I, Devaux E, Laluet J Y and Ebbesen T W 2007 Wavelength selective nanophotonic components utilizing channel plasmon polaritons *Nano Lett.* **7** 880–4
[10] Nielsen R B, Fernandez-Cuesta I, Boltasseva A, Volkov V S, Bozhevolnyi S I, Klukowska A and Kristensen A 2008 Channel plasmon polariton propagation in nanoimprinted *V*-groove waveguides *Opt. Lett.* **33** 2800–2
[11] Zenin V A, Volkov V S, Han Z, Bozhevolnyi S I, Devaux E and Ebbesen T W 2011 Dispersion of strongly confined channel plasmon polariton modes *J. Opt. Soc. Am.* B **28** 1596–602
[12] Zenin V A, Volkov V S, Han Z, Bozhevolnyi S I, Devaux E and Ebbesen T W 2012 Directional coupling in channel plasmon-polariton waveguides *Opt. Express* **20** 6124–34
[13] Dintinger J and Martin O J F 2009 Channel and wedge plasmon modes of metallic *V*-grooves with finite metal thickness *Opt. Express* **17** 2364–74
[14] Lee S and Kim S 2011 Long-range channel plasmon polaritons in thin metal film *V*-grooves *Opt. Express* **19** 9836–47
[15] Vernon K C, Gramotnev D K and Pile D F P 2008 Channel plasmon-polariton modes in V grooves filled with dielectric *J. Appl. Phys.* **103** 034304
[16] Srivastava T and Kumar A 2009 Propagation characteristics of channel plasmon polaritons supported by a dielectric filled trench in a real metal *J. Appl. Phys.* **106** 043104
[17] Moreno E, Garcia-Vidal F J, Rodrigo S G, Martin-Moreno L and Bozhevolnyi S I 2006 Channel plasmon-polaritons: modal shape, dispersion, and losses *Opt. Lett.* **31** 3447–9
[18] Oulton R F, Sorger V J, Genov D A, Pile D F P and Zhang X 2008 A hybrid plasmonic waveguide for subwavelength confinement and long-range propagation *Nature Photon.* **2** 496–500
[19] Bian Y S, Zheng Z, Zhao X, Zhu J S and Zhou T 2009 Symmetric hybrid surface plasmon polariton waveguides for 3D photonic integration *Opt. Express* **17** 21320–5

[20] Dai D X and He S L 2009 A silicon-based hybrid plasmonic waveguide with a metal cap for a nano-scale light confinement *Opt. Express* **17** 16646–53
[21] Bian Y S, Zheng Z, Liu Y, Zhu J S and Zhou T 2010 Dielectric-loaded surface plasmon polariton waveguide with a holey ridge for propagation-loss reduction and subwavelength mode confinement *Opt. Express* **18** 23756–62
[22] Kwon M S 2011 Metal–insulator–silicon–insulator–metal waveguides compatible with standard CMOS technology *Opt. Express* **19** 8379–93
[23] Bian Y S, Zheng Z, Liu Y, Liu J S, Zhu J S and Zhou T 2011 Hybrid wedge plasmon polariton waveguide with good fabrication-error-tolerance for ultra-deep-subwavelength mode confinement *Opt. Express* **19** 22417–22
[24] Kim J T and Choi S-E 2012 Hybrid plasmonic slot waveguides with sidewall slope *IEEE Photon. Technol. Lett.* **24** 170–2
[25] Bian Y S, Zheng Z, Zhao X, Su Y L, Liu L, Liu J S, Zhu J S and Zhou T 2012 Guiding of long-range hybrid plasmon polariton in a coupled nanowire array at deep-subwavelength scale *IEEE Photon. Technol. Lett.* **24** 1279–81
[26] Zhu S Y, Liow T Y, Lo G Q and Kwong D L 2011 Silicon-based horizontal nanoplasmonic slot waveguides for on-chip integration *Opt. Express* **19** 8888–902
[27] Bian Y S, Zheng Z, Zhao X, Su Y L, Liu L, Liu J S, Zhou T and Zhu J S 2012 Hybrid plasmonic structures based on CdS nanotubes: a novel route to low-threshold lasing on the nanoscale *J. Phys. D: Appl. Phys.* **45** 505105
[28] Boltasseva A, Volkov V S, Nielsen R B, Moreno E, Rodrigo S G and Bozhevolnyi S I 2008 Triangular metal wedges for subwavelength plasmon-polariton guiding at telecom wavelengths *Opt. Express* **16** 5252–60
[29] Bian Y S, Zheng Z, Zhao X, Su Y L, Liu L, Liu J S, Zhu J S and Zhou T 2013 Highly confined hybrid plasmonic modes guided by nanowire-embedded-metal grooves for low-loss propagation at 1550 nm *IEEE J. Sel. Top. Quantum Electron.* at press doi:10.1109/JSTQE.2012.2212002
[30] Moreno E, Rodrigo S G, Bozhevolnyi S I, Martin-Moreno L and Garcia-Vidal F J 2008 Guiding and focusing of electromagnetic fields with wedge plasmon polaritons *Phys. Rev. Lett.* **100** 023901
[31] Chen L, Shakya J and Lipson M 2006 Subwavelength confinement in an integrated metal slot waveguide on silicon *Opt. Lett.* **31** 2133–5